

# Hall effect on magnetic reconnection at the Earth's magnetopause

Laura F. Morales<sup>a,\*</sup>, Sergio Dasso<sup>a,b,1</sup>, Daniel O. Gómez<sup>a,b,1</sup>, Pablo Mininni<sup>b</sup>

<sup>a</sup>*Instituto de Astronomía y Física del Espacio, CC. 67, suc. 28, 1428 Buenos Aires, Argentina*

<sup>b</sup>*Departamento de Física, Facultad de Ciencias Exactas y Naturales, Universidad de Buenos Aires, 1428 Buenos Aires, Argentina*

Available online 8 September 2005

## Abstract

We analyze in situ observations of magnetic reconnection at the Earth magnetopause to estimate the importance of the Hall current during the merging of interplanetary and magnetospheric magnetic field lines. The reconnection process is studied through numerical simulations, integrating the Hall MHD equations in 2.5 dimensions. A large influence of the Hall effect is found, which can be measured by a significant increase of the reconnection rate.

© 2005 Published by Elsevier Ltd.

*Keywords:* Magnetosphere; Magnetic reconnection; Hall effect

## 1. Introduction

Conducting plasmas show a tendency to develop thin and intense current sheets where magnetic reconnection can take place. As a result, a sheared magnetic field reverses its sign (inside the so-called “diffusion region”), the magnetic field lines experience topological rearrangements, and part of the magnetic energy is released and converted into kinetic and thermal energy (Parker, 1957). This process of magnetic reconnection can be present in several astrophysical scenarios, such as the magnetopause (Sonnerup et al., 1981), the magnetotail (where it is expected to be the precursor for auroral substorms, see e.g., Birn and Hesse, 1996), the solar atmosphere (related to the occurrence of flares, coronal mass ejections, and coronal heating, see e.g., Priest,

1984; Gosling et al., 1995), or the interplanetary medium (as a consequence of the interaction between magnetic clouds and the solar wind (Farrugia et al., 2001; Schmidt and Cargill, 2003)).

One of the best studied physical scenarios, by in situ observations, is the terrestrial magnetopause, where the magnetic reconnection is responsible for the merging of terrestrial and interplanetary magnetic field lines, thus providing a source of particles, energy, and momentum to the magnetosphere (Sonnerup et al., 1981). The appearance of a kink in the newly reconnected lines produces jets of plasma away from the diffusion region. Although these plasma jets have been previously detected “in situ” by Phan et al. (2000) and Paschmann et al. (1979), observational evidence of the existence of the diffusion regions has been obtained only recently by Mozer et al. (2002).

Hall currents can play a significant role in the dynamics of the fluid and the magnetic fields of many astrophysical objects, such as dense molecular clouds, formation of white dwarfs, or instabilities in accretion disks (Minnini et al., 2003). Due to the low density of the plasma in the solar wind and magnetosphere, the Hall

\*Corresponding author. Fax: +54 11 47868114.

*E-mail addresses:* laura@iafe.uba.ar (L.F. Morales), sdasso@iafe.uba.ar (S. Dasso), gomez@iafe.uba.ar (D.O. Gómez), mininni@df.uba.ar (P. Mininni).

<sup>1</sup>S.D and D.G. are members of the Carrera del Investigador Científico (CONICET).

currents can be of importance during magnetic reconnection at the Earth's magnetopause, and some signatures of the Hall current have been reported (Mozer et al., 2002). More recently, Asano et al. (2004) and Deng et al. (2004) used Geotail observations and identified the spatial structure of a Hall current sheet in the Earth's magnetotail. These studies represent a step forward with respect to earlier observations reported in the literature (Deng and Matsumoto, 2001; Øieroset et al., 2001). However, the relative importance of its contribution to magnetic reconnection have not yet been quantified.

In this work, from in situ plasma and magnetic observations corresponding to the terrestrial magnetopause, we quantitatively assess the importance of the Hall effect in this scenario. We used observations from the spacecraft Equator-S and identified the location and orientation of a current layer. We also determined the relevant plasma parameters at this reconnection site, such as the intensity of the magnetic field, the particle density and the width of the current layer. We also perform numerical simulations to compare the characteristics of a reconnection process with and without the Hall current. To this end, we used the plasma parameters derived from observations to quantify the relevance of the Hall effect.

In Section 2, we present the data analysis, quantifying the importance of the Hall term. The results of our numerical simulations are presented in Section 3, showing a sizeable increase of the reconnection rate when the Hall term is considered. Finally, in Section 4, we list our conclusions.

## 2. Observations

In this section we analyze magnetic observations made by the spacecraft Equator-S with a temporal cadence of 0.5 s, during a magnetopause crossing. On February 11, 1998, Equator-S crossed several times the magnetopause, while the spacecraft Wind simultaneously observed the persistent presence of a southward oriented solar wind magnetic field (Phan et al., 2000), thus providing the proper conditions for magnetic reconnection. More specifically, we report results of a magnetopause crossing starting at 13:32:51 UT and finishing at 13:33:48 UT. The magnetopause crossing is identified by a velocity jump, which in turn, quantitatively corresponds to the difference of the magnetic field components, as emerges from magnetic reconnection theoretical models (Phan et al., 2000).

Since the magnetic field is solenoidal, whenever the spacecraft crosses the thin current layer, along its linear path it records an almost constant perpendicular (to the layer) component of the field, while the tangential component shows a large rotation.

We analyze the three components of the magnetic field vector given in geocentric solar ecliptic (GSE) coordinates. In this reference frame  $\hat{x}_{\text{GSE}}$  corresponds to the Earth–Sun direction,  $\hat{z}_{\text{GSE}}$  points to the north (perpendicular to the ecliptic plane), and  $\hat{y}_{\text{GSE}}$  is such that the system is right handed. The three upper panels of Fig. 1 show these components, with the current layer confined between the dotted vertical lines. In general terms, the magnetopause can be identified by a transition from high-density and southward-field ( $B_{z,\text{GSE}} < 0$ ) in the solar wind to low-density and northward-field in the magnetosphere. However, the detailed structure of these transitions varies from event to event. Also, other physical quantities such as the electrostatic potential or the temperatures jump as well, providing valuable information about the physics involved in these events (see, for instance, Hull et al., 2000).

It is possible to estimate the orientation of the layer by applying the so-called minimum variance (MV) method to the magnetic observations (Sonnerup and Cahill, 1967). This method finds the direction ( $\hat{n}$ ) in which the mean quadratic deviation of the field,  $\langle (\mathbf{B} \cdot \hat{n} - \langle \mathbf{B} \cdot \hat{n} \rangle)^2 \rangle$ , is minimum (maximum). It is possible to show that this is equivalent to finding the eigenvector corresponding to the smallest (highest) eigenvalue of the covariance matrix  $M_{i,j} = \langle B_i B_j \rangle - \langle B_i \rangle \langle B_j \rangle$ . Thus, the MV method determines the direction of the maximum ( $\hat{x}_{\text{layer}}$ ) and minimum ( $\hat{y}_{\text{layer}}$ ) variance of the field, and therefore determines the spatial orientation of the layer.

The two lower panels show  $B_{x,\text{layer}}$  and  $B_{y,\text{layer}}$ , after applying a minimum variance technique to the observations of this event. We find a very good differentiated variance of the components, with a maximum to minimum eigenvalue ratio of about 17, and the normal to the layer being  $\hat{n} = (0.56, -0.73, 0.41)$ , expressed in GSE coordinates.

In Fig. 1 we see that the spacecraft takes 6–8 s to cross the magnetopause. The width of the layer ( $\delta$ ) can be estimated from a normal speed of  $v_n \sim 100$  km/s, thus yielding  $\delta \sim 600$ –800 km.

The Hall term in the induction equation is expected to become significant at length scales smaller or of the order of  $L_H = c/\omega_{\text{pi}}$ , where  $c$  is the speed of the light and  $\omega_{\text{pi}}$  is the ion plasma frequency. The observed proton density in the event considered is  $n_p \sim 5$ –10  $\text{cm}^{-3}$ , and thus the Hall length corresponds to  $L_H \sim 100$  km. Therefore, a priori we can expect the Hall current to produce a non-negligible effect on the reconnection process, since  $L_H/\delta \sim 0.12$ –0.17.

The three upper panels of Fig. 2 show the components of the vector velocity field in the layer-oriented frame. In the upper panel, we show the large change of magnitude of the  $V_{x,\text{layer}}$  component at the magnetopause (the flow tangential acceleration across the reconnection current sheet), while the other two components of the velocity remain almost constant. The last panel of this figure

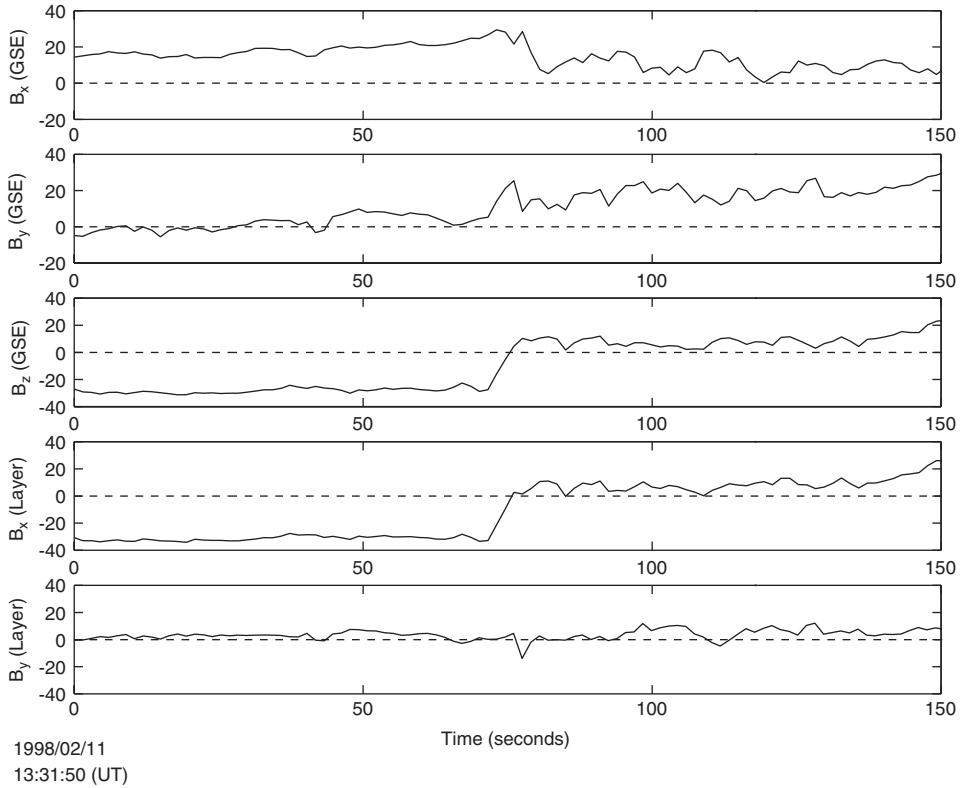


Fig. 1. Magnetic field observations from 13:31:50 to 13:35:00 (UT) on February 11, 1998. From top to bottom: (a) Component  $B_x(t)$  of the magnetic field in GSE coordinates (in nT), (b) Idem  $B_y(t)$ , (c) Idem  $B_z(t)$ , (d) Component of magnetic field tangential to the current layer after applying the minimum variance method, (e) Idem for the perpendicular component.

shows the proton particle density, showing a marked density drop as the spacecraft enters to the magnetosphere.

### 3. Simulation model

When the width of the current layer reaches values of the order of  $L_H$  or lower, it is no longer valid to neglect the Hall term in the generalized Ohm's law (Wang et al., 2000). Including two-fluid effects, Ohm's law can be written as (see also Ma and Bhattacharjee, 2001; Pritchett, 2001; Birn et al., 2001)

$$\mathbf{E} + \frac{1}{c} \mathbf{v} \times \mathbf{B} = \frac{4\pi\eta}{c^2} \mathbf{j} + \frac{1}{ne} \left( \frac{1}{c} \mathbf{j} \times \mathbf{B} - \nabla p_e \right), \quad (1)$$

where  $n$  is the electron and proton density (assuming quasi-neutrality),  $e$  is the charge of the electron,  $\eta$  is the electric resistivity,  $\mathbf{v}$  is the plasma flow velocity,  $p_e$  is the electron pressure and  $\mathbf{j}$  is the electric current density. In this approximation, we are neglecting the electron inertia (i.e. we assume  $m_e = 0$ ). The inclusion of electron inertia gives rise to even smaller spatial scales, of the order of the electron skin depth  $c/\omega_{pe}$  ( $\omega_{pe}$ : electron

plasma frequency, see for instance Drake et al., 1997). Assuming incompressibility (i.e.  $\nabla \cdot \mathbf{v} = 0$ ), we can cast the so-called Hall-MHD equations in their dimensionless form as:

$$\partial_t \mathbf{v} + (\mathbf{v} \cdot \nabla) \mathbf{v} = (\nabla \times \mathbf{B}) \times \mathbf{B} - \nabla p + \frac{1}{R} \nabla^2 \mathbf{v}, \quad (2)$$

$$\partial_t \mathbf{B} = \nabla \times [(\mathbf{v} - \varepsilon \nabla \times \mathbf{B}) \times \mathbf{B}] + \frac{1}{S} \nabla^2 \mathbf{B}, \quad (3)$$

$$\nabla \cdot \mathbf{B} = 0 = \nabla \cdot \mathbf{v}. \quad (4)$$

In Eqs. (2)–(3), we have normalized  $\mathbf{B}$  to a typical magnetic intensity  $B_0$ ,  $\mathbf{v}$  to the Alfvén speed  $v_a = B_0/\sqrt{4\pi m_p n}$  (with  $m_p$  the proton mass), the total gas pressure  $p$  to  $\rho v_a^2$ , and longitudes and times, respectively, to  $L_0$  and  $L_0/v_a$ . The Reynolds number is  $R = L_0 v_a/\nu$  and  $S = L_0 v_a/\eta$  is the Lundquist number. The dimensionless coefficient  $\varepsilon$  is defined as  $\varepsilon = L_H/L_0$ , and measures the relative strength of the Hall effect. The dimensionless electron velocity is

$$\mathbf{v}_e = \mathbf{v} - \varepsilon \nabla \times \mathbf{B}. \quad (5)$$

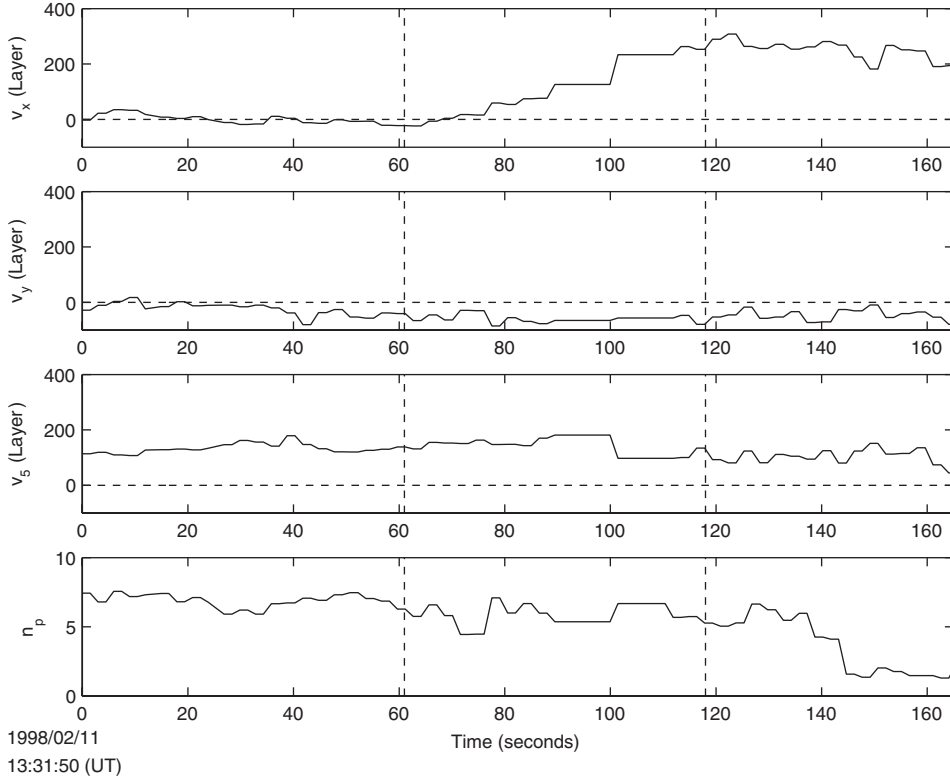


Fig. 2. Velocity (in km/s) and proton density (in particles per  $\text{cm}^{-3}$ ) observations from 13:31:50 (UT) on February 11, 1998.

From Eq. (3) it is apparent that in the non-dissipative limit (i.e.  $S \rightarrow \infty$ ) the magnetic field remains frozen to the electron flow  $\mathbf{v}_e$  rather than to the bulk velocity  $\mathbf{v}$ .

The incompressible Hall MHD simulations reported in this paper are carried out under the geometric approximation known as  $2\frac{1}{2}\text{D}$ . This approximation is based on the assumption that there is translational symmetry along the  $\hat{\mathbf{z}}$  coordinate (i.e.  $\partial_z = 0$ ). Therefore, the solenoidal magnetic and velocity fields, can be represented as

$$\mathbf{B} = \nabla \times [\hat{\mathbf{z}}a(x, y, t)] + \hat{\mathbf{z}}b(x, y, t), \quad (6)$$

$$\mathbf{v} = \nabla \times [\hat{\mathbf{z}}\phi(x, y, t)] + \hat{\mathbf{z}}u(x, y, t), \quad (7)$$

where  $a(x, y, t)$  is the magnetic flux function and  $\phi(x, y, t)$  is the stream function. In this approximation, the Hall MHD equations take the form:

$$\partial_t a = [\phi - \varepsilon b, a] + \frac{1}{S} \nabla^2 a, \quad (8)$$

$$\partial_t b = [\phi, b] + [u - \varepsilon j, a] + \frac{1}{S} \nabla^2 b, \quad (9)$$

$$\partial_t w = [\phi, w] + [j, a] + \frac{1}{R} \nabla^2 w, \quad (10)$$

$$\partial_t u = [b, a] + [\phi, u] + \frac{1}{R} \nabla^2 u. \quad (11)$$

The nonlinearities are expressed in terms of the standard Poisson brackets (i.e.  $[p, q] = \partial_x p \partial_y q - \partial_y p \partial_x q$ ),  $j = -\nabla^2 a$  is the  $\hat{\mathbf{z}}$ -component of the electric current density and  $w = -\nabla^2 \phi$  is the  $\hat{\mathbf{z}}$ -component of the flow vorticity.

We performed numerical integrations of Eqs. (8)–(11). The computation is carried out in a rectangular domain assuming periodic boundary conditions. The spatial coordinates span the ranges  $-\pi \leq x, y \leq \pi$ . The scalar fields  $a(x, y, t)$ ,  $\phi(x, y, t)$ ,  $b(x, y, t)$  and  $u(x, y, t)$  are expanded in their corresponding spatial Fourier amplitudes  $a_k(t)$ ,  $\phi_k(t)$ ,  $b_k(t)$  and  $u_k(t)$ . The equations for these Fourier amplitudes are evolved in time using a second order Runge–Kutta scheme and the nonlinear terms are evaluated following a  $\frac{2}{3}$  dealiased pseudospectral technique. In order to provide a reconnection scenario, the present simulations start with the fluid at rest, and the following initial condition to the field  $\mathbf{B}$ :

$$\mathbf{B}(x, y) = \hat{\mathbf{x}}B_0 \left[ \tanh\left(\frac{y + \pi/2}{\Delta}\right) - \tanh\left(\frac{y - \pi/2}{\Delta}\right) - 1 \right]. \quad (12)$$

Here,  $\Delta = 0.04\pi$  in order to simulate two thin initial current sheets, where the reconnection process takes place. In order to drive reconnection, a monochromatic perturbation with  $k_x = 1$  is added to the initial condition, with an intensity of  $0.02B_0$ . The Reynolds numbers for the runs reported here are  $R = S = 500$  and the spatial size of the simulations is  $256 \times 256$  grid points.

Figs. 3 and 4 show results obtained for cases without the Hall term ( $\varepsilon = 0$ ) and with  $\varepsilon = 0.15$ , in order to simulate similar conditions to those described in Section 2.

In Fig. 3, we present contour plots of the magnetic flux  $a(x, y)$  superimposed to grey levels of  $j$  for the cases  $\varepsilon = 0, 0.15$  when the energy conversion from magnetic to kinetic is maximum (at time  $t = 2$ ). The magnetic flux shows the typical behaviour expected for a two-dimensional magnetic reconnection scenario and it is

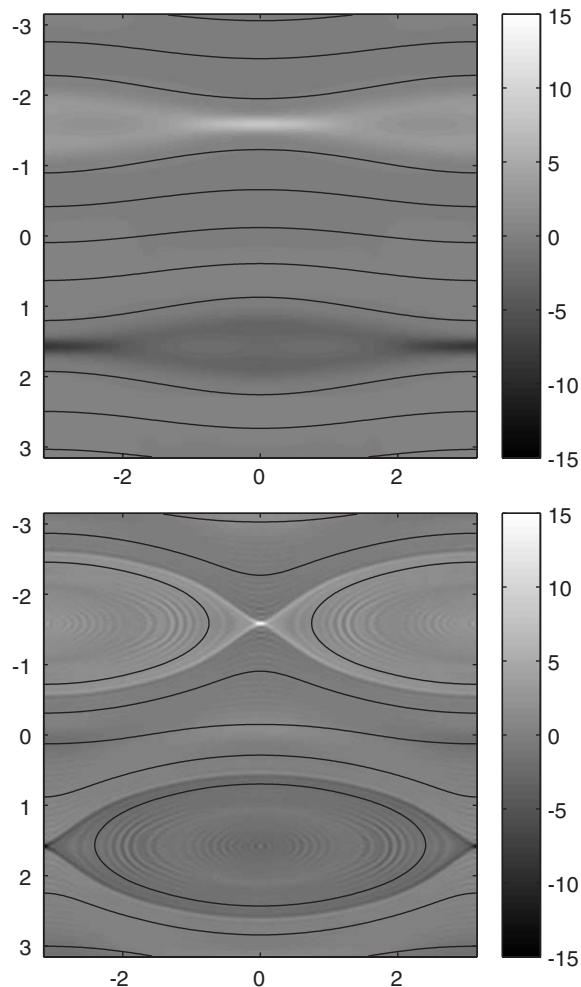


Fig. 3. Contours of magnetic flux  $a(x, y)$  superimposed to grey levels of  $j(x, y)$  at  $t = 2$  for the cases  $\varepsilon = 0$  (above) and  $\varepsilon = 0.15$  (below). The brightest regions correspond to the current sheets.

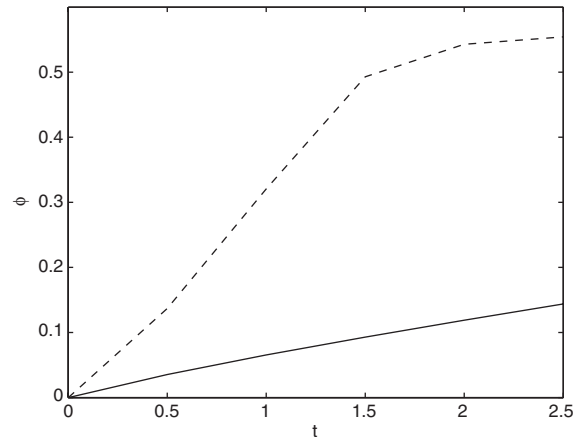


Fig. 4. Total reconnected flux vs. time, for  $\varepsilon = 0$  (solid line) and  $\varepsilon = 0.15$  (dashed line). We compute the total reconnected flux at the X-point, simply as the difference  $\phi(t) = a_X(t) - a_O(t)$ .

possible to see the structure and size of the current sheets. We note that as  $\varepsilon$  increases, the size of the current sheet decreases, as can readily be seen by comparing the  $\varepsilon = 0$  and  $0.15$  cases (see Fig. 3). Consistent with this current structure, the ion flow changes suddenly from the low speed inflow to the much higher speed outflow, in a shock-like fashion reminiscent of Petschek's configuration (see Petschek, 1964; also Shay et al., 1998; Biskamp, 2000).

One of the most important features to evaluate the efficiency of the reconnection process is the total reconnected flux. The magnetic flux reconnected at the X point can be calculated in terms of the difference of the magnetic potential in the X-point and the O-point,  $\phi(t) = a_X(t) - a_O(t)$ . Fig. 4 shows that the reconnection process is significantly faster when the Hall effect is present. Note that even though the strength of the Hall parameter is only  $0.15$ , the reconnected flux at  $t = 2$ , which is the time of maximum energy transfer (from magnetic to kinetic) is about 5 times larger.

#### 4. Conclusions

In this paper, we study the role of the Hall effect in reconnection processes taking place at the Earth's magnetopause. We analyze a particular reconnection event observed by the spacecraft Equator-S, for which we estimate a value for the Hall parameter of  $\varepsilon \sim 0.15$ .

We also present results from numerical simulations within the framework of incompressible Hall MHD in  $2\frac{1}{2}$  dimensions. We compare the resulting structure of the current sheet from the simulations with and without the Hall term. To quantify the relative importance of the Hall term, we used the realistic value of  $\varepsilon \sim 0.15$  derived from observations. Note that the current sheets formed in the presence of the Hall term are much smaller

than those formed when this effect is ignored. We quantify the importance of the Hall effect, as measured by the total reconnected flux, and show that when the Hall term is considered, there is 5 times more reconnected flux.

In summary, our main conclusion is that the Hall effect is crucial during the initial stages of the merging of terrestrial and interplanetary field lines at the magnetopause, inducing a faster reconnection process. Also, the current layer displays different features than those predicted from one-fluid MHD.

### Acknowledgements

The authors thank W. Baumjohann at MPE and the CDAWeb system for facilitating the data used in this paper. This work was supported by the Argentinean Grants UBACyT X209 and X329, CONICET PIP 2693, and PICT 12187 and 14163 (ANPCyT).

### References

- Asano, Y., Mukai, T., Hoshino, M., Saito, Y., Hayakawa, H., Nagai, T., 2004. Current sheet structure around the near-Earth neutral line observed by Geotail. *Journal of Geophysical Research* 109, A02212.
- Birn, J., Hesse, M., 1996. Geospace environment modeling (GEM) magnetic reconnection challenge: resistive tearing, anisotropic pressure and hall effects. *Journal of Geophysical Research* 101, 15345–15358.
- Birn, J., et al., 2001. Geospace environmental modeling (GEM) magnetic reconnection challenge. *Journal of Geophysical Research* 106, 3715–3719.
- Biskamp, D., 2000. *Magnetic Reconnection in Plasmas*, Cambridge Monographs on Plasma Physics. Cambridge University Press, Cambridge.
- Deng, X.H., Matsumoto, H., 2001. Rapid magnetic reconnection in the Earth's magnetosphere mediated by whistler waves. *Nature* 410, 557.
- Deng, X.H., Matsumoto, H., Kojima, H., Mukai, T., Anderson, R.R., Baumjohann, W., Nakamura, R., 2004. Geotail encounter with reconnection diffusion region in the Earth's magnetotail: evidence of multiple X lines collisionless reconnection? *Journal of Geophysical Research* 109, A05206.
- Drake, J.F., Biskamp, D., Zeiler, A., 1997. Breakup of the electron current layer during 3-D collisionless magnetic reconnection. *Geophysical Research Letters* 24, 2921–2924.
- Farrugia, C.J., et al., 2001. A reconnection layer associated with a magnetic cloud. *Advances in Space Research* 28, 759–764.
- Gosling, J.T., et al., 1995. Three-dimensional magnetic reconnection and the magnetic topology of coronal mass ejection events. *Geophysical Research Letters* 22, 869–872.
- Hull, A.J., Scudder, J.D., Fitzenreiter, R.J., Ogielvie, K.W., Newbury, J.A., Russel, C.T., 2000. Electron temperature and deHoffmann–Teller potential change across the Earth's bow shock: new results from ISEE1. *Journal of Geophysical Research* 105, 20957–20971.
- Ma, Z., Bhattacharjee, A., 2001. Hall magnetohydrodynamic reconnection: the geospace environment modeling challenge. *Journal of Geophysical Research* 106, 3773–3782.
- Minnini, P., Gomez, D.O., Mahajan, S.M., 2003. Role of the Hall current in magnetohydrodynamic dynamos. *Astrophysical Journal* 584, 1120–1126.
- Mozer, F., Bale, S., Phan, T.D., 2002. Evidence of diffusion regions at a subsolar magnetopause crossing. *Physical Review Letters* 89, 015002.
- Øieroset, M., et al., 2001. In situ detection of collisionless reconnection in the Earth's magnetotail. *Nature* 412, 414–417.
- Parker, E.N., 1957. Sweet's mechanism for merging magnetic fields in conducting fluids. *Journal of Geophysical Research* 62, 509–520.
- Paschmann, G., et al., 1979. Plasma acceleration at the Earth's magnetopause—Evidence for reconnection. *Nature* 282, 243–246.
- Petschek, H.E., 1964. Magnetic annihilation. In: Ness, W.N. (Ed.), *AAS/NASA Symposium on the Physics of Solar Flares*. National Aeronautics and Space Administration, Science and Technical Information Division.
- Phan, T.D., et al., 2000. Extended magnetic reconnection at the Earth's magnetopause from detection of bi-directional jets. *Nature* 404, 848–850.
- Priest, E.R., 1984. Magnetic reconnection at the Sun. In: Hones, E.W. (Ed.), *Magnetic Reconnection in Space and Laboratory Plasmas*. Geophysical Monograph Series, vol. 30. American Geophysical Union.
- Pritchett, P.L., 2001. Geospace environment modeling magnetic reconnection challenge: Simulations with a full particle electromagnetic code. *Journal of Geophysical Research* 106, 3783–3798.
- Schmidt, J.M., Cargill, P.J., 2003. Magnetic reconnection between a magnetic cloud and the solar wind magnetic field. *Journal of Geophysical Research* 108 (A1), 1023.
- Shay, M., Drake, J.F., Denton, R.E., Biskamp, D., 1998. Structure of the dissipation region during collisionless magnetic reconnection. *Journal of Geophysical Research* 25, 9165.
- Sonnerup, B.U.O., Cahill, L.J., 1967. Magnetopause structure and attitude from explorer 12 observations. *Journal of Geophysical Research* 72, 171.
- Sonnerup, B.U.O., et al., 1981. Evidence for magnetic field reconnection at the Earth's magnetopause. *Journal of Geophysical Research* 86, 10049–10067.
- Wang, X., Bhattacharjee, A., Ma, Z.W., 2000. Collisionless reconnection: effects of Hall current and electron pressure gradient. *Journal of Geophysical Research* 105, 27633–27648.